9918–9932 *Nucleic Acids Research, 2016, Vol. 44, No. 20* *Published online 5 July 2016*
doi: 10.1093/nar/gkw613

Binding properties of YjeQ (RsgA), RbfA, RimM and Era to assembly intermediates of the 30S subunit

Brett Thurlow[1], Joseph H. Davis[2], Vivian Leong[1], Trevor F. Moraes[3], James R. Williamson[2] and Joaquin Ortega[1,*]

[1]Department of Biochemistry and Biomedical Sciences and M.G. DeGroote Institute for Infectious Diseases Research, McMaster University, 1280 Main Street West, Hamilton, Ontario L8S4K1, Canada, [2]Department of Integrative Computational and Structural Biology, The Scripps Research Institute, La Jolla, CA 92037, USA and [3]Department of Biochemistry, University of Toronto, 1 King's College Circle, Toronto, Ontario M5S1A8, Canada

Received December 22, 2015; Revised June 26, 2016; Accepted June 27, 2016

ABSTRACT

Our understanding regarding the function of YjeQ (also called RsgA), RbfA, RimM and Era in ribosome biogenesis has been derived in part from the study of immature 30S particles that accumulate in null strains lacking one of these factors. However, their mechanistic details are still unknown. Here, we demonstrate that these immature particles are not dead-end products of assembly, but progress into mature 30S subunits. Mass spectrometry analysis revealed that *in vivo* the occupancy level of these factors in these immature 30S particles is below 10% and that the concentration of factors does not increase when immature particles accumulate in cells. We measured by microscale thermophoresis that YjeQ and Era binds to the mature 30S subunit with high affinity. However, the binding affinity of these factors to the immature particles and of RimM and RbfA to mature or immature particles was weak, suggesting that binding is not occurring at physiological concentrations. These results suggest that in the absence of these factors, the immature particles evolve into a thermodynamically stable intermediate that exhibits low affinity for the assembly factors. These results imply that the true substrates of YjeQ, RbfA, RimM and Era are immature particles that precede the ribosomal particles accumulating in the knockouts strains.

INTRODUCTION

The bacterial 70S ribosome is made of two subunits designated as the 30S (or small) and 50S (or large) subunits. The 30S subunit (SSU) is comprised of the 16S ribosomal RNA (rRNA) molecule and 21 ribosomal proteins (r-proteins) and its main role during translation is the decoding of the mRNA (1,2). The 50S subunit (LSU) contains two rRNA molecules, the 23S and 5S rRNAs and 34 r-proteins and its main function is to catalyze peptide bond formation during protein translation (3–5). Much is now understood about the structure of the ribosome and the dynamic conformational changes that this macromolecular complex undergoes during protein translation (3,6,7). However, how this massive ribonucleoprotein complex assembles within cells remains elusive.

Assembly of the 30S subunit is a complex process characterized by the existence of multiple events occurring simultaneously (8,9). The rRNA starts to fold as soon as the 5′ end of the primary rRNA transcript is synthesized (10,11). Concurrently, the r-proteins associate in a hierarchical manner directing the folding of the rRNA (2). Modifications of the r-proteins and rRNA (12), as well as the processing of the rRNA by RNases (13–16) are simultaneously occurring during rRNA folding. Recent kinetic work has revealed that assembly of the ribosomal subunit occurs through multiple parallel pathways with numerous rate-limiting steps (17–20). These multiple pathways introduce the necessary flexibility and redundancy to make ribosome assembly an extremely robust and efficient process.

Our study focuses on the maturation events catalyzed by four protein factors: YjeQ (also know as RsgA), RbfA, RimM and Era (21–26). YjeQ and Era are GTPases, but RbfA and RimM do not exhibit a measurable enzymatic activity.

Characterization of several late 30S assembly intermediates that accumulate in *Escherichia coli* cells lacking either YjeQ (22), RimM (27,28) or RbfA (29,30) revealed that the immature 30S particles that accumulate in these null strains are structurally similar. Most of the structural motifs of these ribosomal subunits resemble those of the mature 30S subunit, however they all present a severe distortion at the decoding center that renders these ribosomal particles unable to associate with the 50S subunit and engage in translation. Based on these observations, it was postu-

*To whom correspondence should be addressed. Tel: +1 905 525 9140 (Ext 22703); Fax: +1 905 522 9033; Email: ortegaj@mcmaster.ca

lated that YjeQ, RbfA, RimM and Era bind these immature 30S particles at or near the decoding center to assist in its folding (23,24,26,31). However, the nature of the immature 30S particles that the Δ*yjeQ*, Δ*rimM or* Δ*rbfA* knockout strains accumulate and whether they represent true on-pathway assembly intermediates is still unknown. It is also unclear whether YjeQ, RbfA, RimM and Era bind to these assembling 30S particles.

To address these questions we purified mature 30S subunits and the immature 30S particles that accumulate in Δ*yjeQ* ($30S_{\Delta yjeQ}$) and Δ*rimM* ($30S_{\Delta rimM}$) *E. coli* strains. We demonstrated using pulse-chase experiments and *in vitro* maturation assays that these immature particles are not dead-end products of assembly and still progress into mature 30S subunits that assemble into 70S ribosomes, however, maturation occurs at a much slower pace in the absence of YjeQ or RimM. Quantitative mass spectrometry analysis (qMS) revealed these immature 30S subunits when purified under non-dissociating conditions bore low or undetectable concentrations of bound factors. Analyzing the factor protein levels in cell lysates of parental and null strains showed that the concentration of factors does not appreciably increase when immature particles accumulate in the cell. We then measured the binding affinity of YjeQ, Era, RimM and RbfA to the $30S_{\Delta yjeQ}$ and $30S_{\Delta rimM}$ immature particles and the mature 30S subunit using microscale thermophoresis. We found that YjeQ and Era bind to the mature 30S subunit with high affinity, but their binding affinity to $30S_{\Delta yjeQ}$ and $30S_{\Delta rimM}$ was much lower. In the case of RimM and RbfA, we found that their binding affinity to the 30S subunit and immature subunits was either weak or binding was not detected.

These results suggest that the conformations reached by the immature ribosomal particles that are recognized by YjeQ, Era, RimM and RbfA are likely thermodynamically unstable. In the absence of the assembly factors, the immature particles evolve into a more energetically stable conformation with low affinity for the assembly factors. Interestingly, the presented data indicates that the actual substrates for YjeQ, Era, RimM and RbfA are assembly intermediates at earlier stages of the maturation process than the immature ribosomal particles that accumulate in the Δ*yje*Q and Δ*rimM* null strains.

MATERIALS AND METHODS

Cell strains and protein overexpression clones

Parental *E. coli* K-12 (BW25113), Δ*yje*Q and Δ*rimM* null strains were obtained from the Keio collection, a set of *E. coli* K-12 in-frame, single gene knockout mutants (32).

The high copy plasmids pCA24N, pCA24N-*rimM* and pCA24N-*yjeQ* were obtained from the ASKA collection, which contains a complete set of open reading frame clones of *E. coli* (33). These vectors express N-terminal histidine-tagged RimM and YjeQ respectively under the control of isopropyl- beta-D-thiogalactopyranoside-inducible promoter $P_{T5\text{-}lac}$.

The pDEST17-*yjeQ* plasmid used to overexpress YjeQ protein with a N-terminal His_6 tag cleavable by tobacco etch virus (TEV) protease was generated as previously described (23). The pET15b-*rbfA* plasmid used to overexpress RbfA with a N-terminal His_6 tag cleavable by thrombin protease was produced as previously described (34).

Plasmid pET15b-*rimM* and pET15b-*era* used for overexpression of RimM and Era were produced, respectively as follows. The sequence of the *rimM* gene (NCBI reference sequence: NC_010473.1) and *Era* gene (GenBank reference: AP009048.1) were optimized for overexpression in *E. coli* cells using the GeneOptimizer software® and subsequently synthesized (Life Technologies; Thermo Fisher Scientific) with a NdeI and a BamHI site in the 5′ and 3′ ends of the gene, respectively. The genes were cloned into the carrier pMA-T plasmid using the *SfiI* and *SfiI* cloning sites and subsequently subcloned into the final expression vector pET15b using the NdeI and a BamHI restriction sites. The resulting pET15b-*rimM* and pET15b-*era* plasmids produce the RimM and Era protein with a N-terminal His_6 tag cleavable by thrombin. We used sequencing (MOBIX, McMaster University) to validate all overexpression clones.

Protein overexpression and purification

YjeQ was overexpressed as a N-terminal His_6-tag protein by transforming *E. coli* BL21-A1 with the pDEST17-*yjeQ* plasmid described above. Era, RimM and RbfA were overexpressed as N-terminal His_6-tag proteins by transforming *E. coli* BL21-DE3 with pET15b-*Era,* pET15b-*rimM* or pET15b-*rbfA* plasmids, respectively.

The overexpression protocol as well as the harvesting and lysis of the cells prior to protein purification, was performed for the four proteins in a similar manner. Typically, one liter of LB medium was inoculated with 10 ml of saturated overnight culture and cells were grown to $OD_{600} = 0.6$ by incubation at 37°C and shaking at 225 rpm in an Excella E24 incubator (New Brunswick). Expression was induced with 0.2% L-arabinose for YjeQ or 1 mM IPTG for Era, RimM and RbfA. Cells were then induced for 3 h at 37°C and harvested by centrifugation at 3700*g* for 15 min. Cell pellets were washed with 1× PBS buffer (137 mM NaCl, 2.7 mM KCl, 8.1 mM Na_2HPO_4 at pH 7.4) and resuspended in 20 ml of lysis buffer (50 mM Tris–HCl at pH 8.0, 10% [w/v] sucrose, 100 mM NaCl) containing a protease inhibitor cocktail (Complete Protease Inhibitor Cocktail Tablets. Roche). The cell suspension was passed through a French pressure cell at 1400 kg/cm^2 three consecutive times to lyse the cells. The lysate was spun at 39 200*g* for 45 min to clear cell debris and the supernatant was collected. All of the following steps were performed at 4°C.

In the case of the Era protein, the purification process started with drop-wise addition of a 5% polyethyleneimine (PEI) solution to the lysate with shaking to a final concentration of 0.0175% [v/v]. After centrifugation at 1200*g* for 10 minutes in an Eppendorf Mini-spin centrifuge, the soluble portion was recovered. Saturated ammonium sulfate (AS) (4.1 M) solution was then added drop-wise while the solution was shaking until a concentration of 45% AS [v/v] was reached. The precipitate that formed was collected and dissolved in ∼10 ml of buffer containing 50 mM Tris–HCl at pH 8.0, 0.5 M NaCl and 5% [v/v] glycerol. The purification of Era then proceeded using a combination of metal chelating and anion exchange chromatography (see below). In the case of YjeQ, RimM and RbfA the purifi-

cation was performed in the same manner, but without the initial polyethyleneimine and AS precipitation steps.

To this end, NaCl was added to the supernatant of the YjeQ, RimM and RbfA overexpressing cells to a concentration of 0.5 M. Clarified cell lysates of all four assembly factors were passed through a 0.45-μm syringe filter (Millipore) and loaded onto a HiTrap Metal Chelating Column (GE Healthcare Life Sciences) previously equilibrated with 50 mM Tris–HCl at pH 8.0, 0.5 M NaCl and 5% [v/v] glycerol. Nonspecifically bound proteins were washed with incremental step-wise increases in the concentration of imidazole from 45 mM to 90 mM for YjeQ, Era and RimM and 30 mM and 75 mM for RbfA. YjeQ, RimM and RbfA were eluted with 240 mM imidazole and Era with 255 mM imidazole. Purity of the fractions was monitored by SDS-PAGE and fractions containing each respective protein were collected and pooled together.

For YjeQ, the N-terminal His_6-tag was removed by digestion with TEV protease at a ratio of 10:1 (YjeQ:TEV) during overnight dialysis against buffer containing 50 mM Tris–HCl at pH 8.0, 60 mM imizadole and 0.2 M NaCl. Any overnight precipitate was removed by spinning at 12 000*g* for 10 min and the supernatant was collected and loaded onto a HiTrap Metal Chelating Column previously equilibrated with 50 mM Tris–HCl at pH 8.0, 0.2 M NaCl and 60 mM imidazole. Fractions were collected and their purity evaluated by SDS-PAGE and Coomassie Brilliant Blue staining. Fractions containing pure untagged YjeQ were pooled and dialyzed against 50 mM Tris–HCl at pH 8.0, 5% [v/v] glycerol overnight. To concentrate the protein we used a 10 kDa-cutoff filter (Amicon) and the purified YjeQ was frozen in liquid nitrogen and stored at −80°C.

For Era, RimM and RbfA the N-terminal His_6-tag was removed by digestion with thrombin (Sigma) at a concentration of 10 U/mg during overnight dialysis against 50 mM Tris–HCl at pH 8.0, 5% [v/v] glycerol. In the case of the RbfA protein used for the filtration assays, the pooled fractions were dialyzed overnight against 50 mM Tris–HCl at pH 8.0, 5% [v/v] glycerol. However, the N-terminal His_6-tag in RbfA was not removed to allow for easier visualization of the protein with the 30S ribosomal subunits on the bis-tris gels. Dialyzed protein preparations were spun at 12 000*g* for ten minutes in an Eppendorf Mini-spin centrifuge to remove any precipitated protein. Supernatant was collected and loaded onto a Hi-Trap Q HP anion exchange column (GE Healthcare Life Sciences) previously equilibrated with 50 mM Tris–HCl at pH 8.0, 5% [v/v] glycerol. RimM was washed with a linear NaCl gradient and was eluted between 350–500 mM NaCl. RbfA was washed with 50 mM NaCl and then eluted with 100 mM NaCl. An incremental step-wise increase in NaCl concentration at 50 and 150 mM was used to wash Era and this protein was eluted with 450 mM NaCl. We used SDS-PAGE stained with Coomassie Brilliant Blue to evaluate the purity of the eluted fractions containing Era, RimM or RbfA. Fractions containing pure protein were pooled, dialyzed against 50 mM Tris–HCl at pH 8.0, 5% [v/v] glycerol overnight and concentrated using a 10 kDa-cutoff filter (Amicon). Pure proteins were frozen in liquid nitrogen and stored at −80°C.

To obtain ^{15}N-labeled proteins for mass spectrometry analysis, the assembly factors were purified as described above with the following modifications to the growth conditions. A mixture containing 2.5 ml of LB media and 2.5 ml of M9 minimal media containing 18.7 mM $^{15}NH_4Cl$ was inoculated with *E. coli* cells transformed with the overexpression plasmids pDEST17-*yjeQ*, pET15b-*era*, pET15b-*rbfA* or pET15b-*rimM*. The cells were grown for 8 h at 37°C with shaking at 225 rpm until cultures reached turbidity. Saturated cultures were then inoculated into 100 ml of M9 minimal media containing 18.7 mM $^{15}NH_4Cl$ and grown overnight at 37°C with shaking at 225 rpm. A volume of 900 ml of fresh M9 minimal media containing 18.7 mM $^{15}NH_4Cl$ was then inoculated with 100 ml of the saturated overnight culture and cells were grown at 37°C with shaking at 225 rpm until they reached to $OD_{600} = 0.6$. All subsequent steps for the protein over-expression, lysing and harvesting of cells and purification of the ^{15}N-labeled assembly factors were performed as described above. For mass spectrometry analysis, the N-terminal His_6-tag was removed in all four proteins including RbfA.

Purification of 30S ribosomal subunits

Purified 30S subunits from wild type (BW25113), *yjeQ* and *rimM E. coli* null strains were prepared using ultracentrifugations over sucrose cushions and gradients as previously described (27). For the *yjeQ* and *rimM E. coli* null strains, 4 liters of LB media were inoculated with 40 ml of saturated overnight culture and cells were grown at 37°C with 225 rpm of shaking in an Excella E24 incubator (New Brunswick) to an OD_{600} of 0.2. For the wild type strain, 1 l of LB media was grown in a similar manner to an OD_{600} of 0.6. Cells were cooled down to 4°C and all subsequent steps were conducted at this temperature as described in (27).

In the case of the 30S subunits purified under 'low salt conditions' for mass spectrometry analysis we used a similar protocol as described in (27), however, all buffers A to F contained only 60 mM NH_4Cl. In addition, the high salt wash performed in buffer C was omitted.

Analysis of the rRNA in the $30S_{\Delta yjeQ}$ and $30S_{\Delta rimM}$ particles

In the experiment where we analyzed the rRNA content in fractions of the sucrose gradients (Figure 1A), fractions containing the free 30S, free 50S and 70S ribosomes were collected independently. Fractions for each subunit were pooled together and the ribosomal particles pelleted overnight at 120,000*g*. Pellets were resuspended in 80 μl of water, and the concentration was determined. Volume was adjusted to 100 μl and we ensured that the total amount of rRNA did not exceed 100 μg. Proteinase K was added to a final concentration of 100 μg/ml and the mixture was incubated at room temperature for 30 min. We then added 350 μl of RLT buffer from Qiagen RNeasy mini isolation kit and 250 μl of 100% ethanol. The reaction was mixed and loaded on the column provided by the Qiagen RNeasy mini isolation kit. Subsequent washes of the column were done according to the manufacture's protocol. RNA Loading Dye 2X (ThermoScientific) was added to 2 μg of purified rRNA samples, heated at 70°C for 10 min and put on ice for 5 min before loading into a modified agarose gel containing 0.7% agarose and 0.9% Synergel (Diversified Biotech)

in 0.5× TBE buffer. RNA was separated by electrophoresis and visualized under UV light.

Pulse-chase labeling experiments

Cultures of wild type (BW25113), Δ*yje*Q and Δ*rim*M *E. coli* strains were grown overnight at 37°C with shaking at 225 rpm to saturation in modified AB minimal media without uracil. We used 0.5 ml of each overnight culture to inoculate 50 mL of fresh AB media without uracil and these cultures were grown to mid-log phase. IPTG was added where indicated at the beginning of the 'chase' phase of the experiment at the concentrations shown in Figure 1. Cells were harvested by centrifuging at 5300*g* for 10 min in a conical tube and resuspended with 1 ml of modified AB media without uracil. We incubated cells at 37°C with shaking at 225 rpm for 5 min to let them equilibrate and then 125 μCi of ^{3}H (tritium) uracil were added to the conical tube for a 2 min pulse at 37°C. Subsequently, to perform the chase 200 μl samples of the culture were removed and added to multiple conical tubes each containing 4 ml of AB media with 8.9 mM uracil. At each time point of the chase 420 μl of phenol–ethanol solution (5% water–saturated phenol, 95% ethanol) was added to the conical tubes to stop rRNA processing. To harvest the cells, samples collected from all time points were spun at 5300*g* for 5 min, flash frozen in liquid nitrogen and stored at −20°C for subsequent rRNA analysis. Total RNA was extracted using the RNeasy Mini Kit (Qiagen) according to the manufacture's protocol. Isolated total RNA was loaded onto an 8% urea + 4% polyacrylamide gel and subjected to electrophoresis. The gel was washed in 0.5× Tris-buffered saline (TBS) and transferred to an Immobilon-Ny+ nylon membrane (Millipore) using electrophoresis. The nylon membrane was cross-linked by baking at 80°C for 2 h, sprayed with En^{3}hance Spray (PerkinElmer) and placed in a BioMax TranScreen-LE intensifying screen (Kodak) with BioMax MS film (Kodak). The BioMax Cassette (Kodak) was placed at −80°C for ∼96 h and the film was developed.

In vitro ribosome subunit maturation assay

In vitro maturation of 30S subunits was observed by monitoring the association of 30S subunits with 50S subunits to form 70S ribosomes. Crude ribosomes were prepared from wild type, Δ*yje*Q and Δ*rim*M *E. coli* strains by inoculating 1 l of LB media with 10 ml of saturated overnight culture. Cells were grown at 37°C with 225 rpm of shaking to mid log phase. Cells were cooled down to 4°C and all subsequent steps were performed at this temperature unless otherwise noted.

Cultures were harvested by centrifugation at 3300*g* for 15 min and the cell pellet was washed in buffer QPA (10 mM Tris–HCl, pH 7.5, 10.5 mM $MgCl_2$, 60 mM KCl). Cells were centrifuged at 3400*g* for 15 min and resuspended in 6 ml lysis buffer (10 mM Tris–HCl, pH 7.5, 10.5 mM $MgCl_2$, 60 mM KCl, 0.5% Tween 20 (v/v) and 1 mM dithiothreitol (DTT)) with the addition of Complete Mini protease inhibitor cocktail and DNaseI (Roche). We performed the cell lysis by passing the suspension through a French pressure cell at 1400 kg/cm^2 three consecutive times. Cellular debris was clarified by spinning the lysate at 27 700*g* for 20 min. Recovered supernatant was loaded into an Amicon Ultra 10 kDa MWCO filter (Millipore) and spun at 3400*g* for 25 min to concentrate the volume to ∼1 ml. The concentrated cell lysate was then divided into equal volumes for subsequent treatments and incubated at 37°C or 4°C for 1 or 2 h, as indicated in Figure 2. After the treatment, cell lysates were subjected to ultracentrifugation at 386 400*g* for 45 min and the pellet gently washed by rinsing in 500 μl of buffer QPB (20 mM Tris–HCl, pH 7.5, 6 mM $MgCl_2$, 30 mM NH_4Cl, 1mM DTT). Subsequently, the pellet containing the crude ribosomes was resuspended in 250 μl of buffer QPB. Then, an equal volume of buffer QPC (20 mM Tris–HCl, pH 7.5, 6 mM $MgCl_2$, 800 mM NH_4Cl, 1 mM DTT) was added for a stringent high salt wash and the mixture was rocked at 4°C for 1 h. The mixture was then clarified by spinning at 31 900*g* for ten min and the supernatant was collected. Crude ribosomes were pelleted by spinning at 386 400*g* for 45 min and the pellet was gently washed by rinsing it and then resuspending it in 500 μl of buffer QPD (20 mM Tris–HCl at pH 7.5, 10 mM $MgCl_2$, 30 mM NH_4Cl, 1 mM DTT) for 1 h. The crude ribosomes were clarified by spinning at 31 900*g* for 10 min and the supernatant was collected.

A portion of the crude ribosome suspension (10A_{260} units) was layered onto a 10 ml 10–30% (w/v) sucrose gradient made in buffer QPE (20 mM Tris–HCl at pH 7.5, 10 mM $MgCl_2$, 50 mM NH_4Cl, 1mM DTT) and centrifuged at 48 400*g* for 16.5 h. Gradients were fractionated using an AKTA prime purification system (GE Healthcare) and the elution peaks corresponding to 30S, 50S and 70S particles were monitored by absorbance at A_{260}. The areas under each respective peak were integrated using PrimeView Evaluation software and the total area for all three peaks was normalized for each data set. The proportions of free subunits and absolute value of 70S ribosomes were calculated. The area of the 30S peak plus one-third the area of the 70S peak corresponds to the total 30S population. The area of the 50S peak plus two-thirds the area of the 70S peak corresponds to the total 50S population. The standard deviations calculated for the maturation assays were obtained from three replicas of the experiment.

Quantitative mass spectrometry

Subunit r-protein and assembly factor occupancy were measured in duplicate using either 6 pmol (replicate 1) or 12 pmol (replicate 2) of the subunit. Each ^{14}N-labeled subunit (wild-type 30S, wild-type 70S, $30S_{\Delta rimM,}$ or $30S_{\Delta yjeQ}$) was mixed with 6 pmol of ^{15}N-labeled 70S particles as well as 6 pmol of ^{15}N-labeled RimM, YjeQ, Era, and RbfA proteins. These 'spiked' samples were then precipitated by addition of 13% TCA, pellets were sequentially washed with 10% TCA and acetone as described previously (35). Pellets were then resuspended in 55 μl buffer DB [100 mM NH_4CO_3, 5% acetonitrile, 5 mM dithiotreitol] and incubated for 10 min at 65°C. Iodoacetamide was added to a final concentration of 10 mM and samples were incubated at 30°C for 30 minutes before addition of 0.5 μg trypsin and overnight incubation at 37°C. Tryptic peptides were then purified on C-18 PepClean columns (Pierce).

Tryptic peptides analyzed on an AB/Sciex Triple-TOF 5600+ mass spectrometer coupled to an Eksigent nano-HPLC. Briefly, peptides were loaded onto a 200 μm × 0.5 mm ChromXP C18-CL 3 μm 120 Å trap column using 95% mobile phase A [0.1% v/v formic acid in water], 95% mobile phase B [0.1% v/v formic acid in acetonitrile]. A 2 h concave gradient ranging 5–45% mobile phase B was then run over the aforementioned trap column and a subsequent 75 μm × 15 mm ChromXP C18-CL 3 μm 120 Å analytic column.

A custom MRM-HR mass spectrometry method targeting multiple peptides for each ribosomal protein as well as the assembly factors was developed using Skyline software (University of Washington) (36) as well as spectral data from prior 'discovery' mass spectrometry analyses of ribosomal proteins (37) and purified assembly factors. Peptides were chosen that gave strong MS^1 and MS^2 signals, generally lacked spectral interference, and spanned the elution gradient, allowing for efficient retention time-based scheduling. After filtering on these criteria, 286 precursor ions were selected for analysis. A single method using 7.5 min scheduling windows, which included a 200 ms MS^1 scan (400–1250 m/z) with up to 40 successive 100 ms MS^2 scans (100–1800 m/z) was then used to analyze each sample.

Precursor and product ion chromatograms were extracted using Skyline, filtered for spectral interference and the final peptide measurements were plotted using a series of custom Python scripts (38).

Filtration binding assays

Initially, 100 kDa Nanosep Omega centrifugal devices (PALL) were prepared by blocking for non-specific binding of proteins by incubating the filter membrane with 500 μl of 1% [w/v] bovine serum albumin (BSA) for 90 min. Filters were then washed by rinsing with 500 μl of RNase free water and then removing any residual blocking solution by adding 500 μl of RNase free water and spinning at 12 000*g* for 10 min. Binding reactions were prepared by incubating 200 pmol of each assembly factor (RimM or RbfA) with 40 pmol of mature 30S subunits or immature 30S particles in a 100 μl reaction in Binding Buffer (10 mM Tris–HCl at pH 8.0, 7 mM magnesium chloride, 300 mM NH_4Cl, 1 mM DTT). Reactions were incubated at 37°C for 30 min followed by centrifugation in the blocked 100 kDa Nanosep Omega centrifugal devices (PALL) at 12 000*g* for 10 min to separate 30S particles and 30S-bound proteins that were retained by the filter from unbound proteins in the flow-through (FT) fraction. The flow-through was collected and the filter was gently washed twice with 100 μl of Binding Buffer followed by a 5 min spin at 12 000*g*. Finally, the 30S particles and 30S-bound proteins retained by the filter were vigorously resuspended in 100 μl of Binding Buffer and collected as the bound fraction (B). To resolve the flow-through and bound fractions, 30 μl of sample were mixed with 6× SDS-PAGE loading buffer and loaded into a 4–12% Criterion™ XT Bis-Tris gel (Bio-Rad). Samples were run in XT MOPS buffer (Bio-Rad). Gels were stained with Coomassie Brilliant Blue and visualized using a ChemiDoc MP system (Bio-Rad).

Pelleting assays

Reactions were prepared by mixing 350 pmol of YjeQ (7 μM) with 50 pmoles of 30S particle (1 μM) in a 50 μl reaction in Binding Buffer (10 mM Tris–HCl at pH 8.0, 7 mM magnesium chloride, 300 mM NH_4Cl, 1 mM DTT) with 1 mM GMPNP. Reactions were incubated at 37°C for 30 min. Following incubation, reactions were laid over a 150 μl 1.1 M sucrose cushion in binding buffer and subsequently ultracentrifuged at 436 000*g* for 3.5 h. The supernatant (S) containing free protein that did not pellet with the 30S subunits was collected. The pellet (P) containing the 30S particles and 30S-bound proteins was resuspended in 200 μl of Binding Buffer. To resolve the supernatant and pellet fractions, 30 μl of samples were mixed with 6× SDS-PAGE loading buffer and loaded into a 4–12% Criterion™ XT Bis–Tris gel (Bio-Rad). Samples were run in XT MOPS buffer (Bio-Rad). Gels were stained with Coomassie Brilliant Blue.

Microscale thermophoresis

Microscale thermophoresis is an immobilization free biomolecular interaction technique that exploits how any change in the hydration shell, size or charge of a molecule due to an association with another molecule affects its ability to move along a temperature gradient. This change in the thermophoretic mobility can then be used to determine a dissociation constant, K_d. Initially, a 2–7 μM solution of mature 30S subunits ($30S_{wt}$) or immature 30S ($30S_{\Delta yjeQ}$ or $30S_{\Delta rimM}$) subunits were fluorescently labeled with maleimide red on cysteine residues using the Monolith NT™ Protein Labeling Kit with the addition of 10 mM Mg acetate added to the supplied labeling buffer. Labeling efficiency was ∼0.5:1 (fluorescent label:ribosome particle). This value was obtained by measuring the molar concentrations of the ribosomal particle at A_{260} and the fluorescent label at A_{650}.

For a typical MST experiment, a titration series of 16 dilutions was prepared in 0.5 ml Protein LoBind eppendorf tubes. The concentration of fluorescently labeled 30S subunit was kept constant between 10 and 40 nM and the concentration of titrant was varied. Prior to the preparation of the titration series all samples were centrifuged at 14 000*g* for 10 min to remove any aggregates. A 1:1 serial dilution of non-labeled titrant was then prepared in MST buffer (20 mM Tris–HCl pH 7.5, 150 mM NaCl, 10 mM $MgCl_2$, 1 mM DTT, 0.05% Tween-20, 0.4 mg/ml BSA) at the concentrations specified. For the experiments involving the addition of nucleotide, a concentration of either 1 mM GMP–PNP or GDP was used where indicated. Ten microliters of the serial dilution of the non-labeled assembly factor was mixed with 10 μl of the fluorescently labeled 30S subunit and reactions were incubated for 10 min. Mixed samples were then loaded into hydrophobic glass capillaries (NanoTemper Technologies) and MST analysis was performed using the Monolith NT.115 microscale thermophoresis instrument (NanoTemper Technologies) at ambient temperature. Typically, an LED power of 60–80% and an MST power of 20–60% were used. The resulting binding curves were obtained by plotting the normalized fluorescence (F_{norm} (‰) $= F_1/F_0$) versus the logarithm of different assembly factor concentrations. K_ds were calculated using the NanoTemper

analysis software (version 1.5.41). All experiments were performed in triplicate or greater.

GTPase assays

To measure the intrinsic GTPase activity of YjeQ and Era we incubated a constant concentration of 4 or 2 μM of each protein respectively, with a range of GTP concentrations from 2 to 250 μM. The background of the assay itself was measured by running control reactions with no YjeQ or Era at each GTP concentration. These background values were subtracted from the total GTPase activity exhibited by the reactions containing the assembly factor at each GTP concentration. Reactions to test the stimulation of YjeQ and Era GTPase activity by ribosomal particles contained 50 nM concentration of YjeQ or Era and an equal concentration of either mature 30S subunits or one of the immature particles. All assays were performed by first calculating the background GTPase stimulation from the ribosomal particles at 50 nM incubated with 2 to 250 uM of GTP. This background subtraction was performed for each ribosomal particle to ensure accuracy in the calculations by removing all background phosphate production not due to the assembly factors themselves. All reactions were incubated at 37°C for 30 min before measuring the released free phosphate by the malachite green assay (BioAssays Systems). The assay showed a linear behaviour for this incubation time. Reactions were performed in the reaction buffer (50 mM Tris–HCl (pH 7.5), 200 mM KCl, 10 mM $MgCl_2$ and 1 mM DTT) and terminated by the addition of malachite green reagent. Released phosphate was detected by monitoring the color formation at 620nm using a 96-well plate reader (Tecan Sunrise). The values of K_m and k_{cat} were calculated by fitting the data to the Michaelis–Menten equation using non-linear regression in GraphPad Prism. The assays were performed in triplicate.

RESULTS

Immature 30S ribosomal subunits that accumulate in the *yjeQ* and *rimM* null strains are competent for maturation

We first tested whether the $30S_{\Delta yjeQ}$ and $30S_{\Delta rimM}$ particles were true assembly intermediates that are competent for maturation or instead, were dead-end products of the assembly pathway. In the Δ*yje*Q and Δ*rim*M strains, the 17S rRNA is contained exclusively in the immature 30S particles and all of the 16S rRNA is found within the mature 70S ribosomes (Figure 1A). This is consistent with previous literature (22,25,27,39) characterizing these strains. Therefore, we used the amount of 17S/16S rRNA as a proxy to estimate the proportion of immature 30S subunits that progressed to mature 30S subunits (Figure 1B and C).

In these experiments, a discrete population of 17S rRNA that accumulated in the Δ*yjeQ,* Δ*rimM* and wild-type strains was labeled by adding ^{3}H (tritium)-uracil to the growing culture. Following a two-minute 'pulse,' unlabeled uracil was added to the culture ('chase') and samples were harvested at the indicated time points. The total rRNA in these samples was extracted and resolved with gel electrophoresis (Figure 1B and C). If the immature 30S particles were dead-end products of the assembly process, their 17S rRNA would not be expected to undergo further maturation and thus, it should persist over the time-course as 17S rRNA or would disappear due to degradation and recycling. In contrast, if the accumulated 30S subunits progress

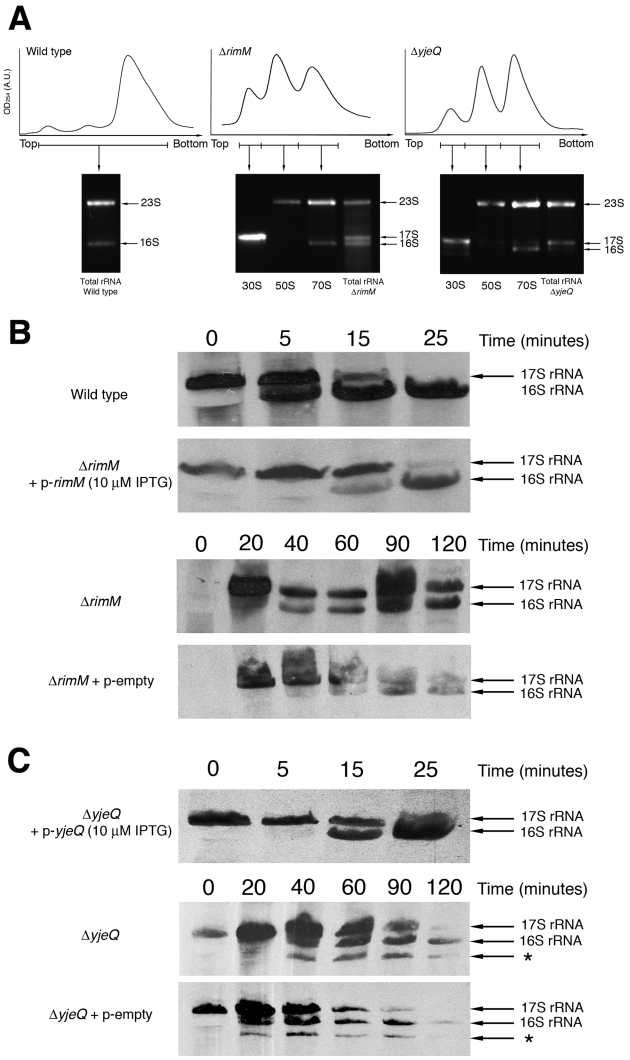

Figure 1. Progress of radiolabeled 17S rRNA in the *yjeQ* and *rimM* null strains. (**A**) The immature $30S_{\Delta yjeQ}$ or $30S_{\Delta rimM}$ particles accumulating in the Δ*yjeQ* and Δ*rimM* strains contain exclusively unprocessed 17S rRNA. Ribosomes from wild type, *yjeQ* and *rimM* null strains were resolved on 10–30% sucrose gradients. Fractions from each peak of the sucrose gradients were collected for total rRNA extraction and resolved by modified agarose gel electrophoresis. Total rRNA content in the three strains was also determined as a control. Gels were stained with ethidium bromide. (**B**) Cells were grown at 37ºC with shaking and then pulsed with 125 μCi of ^{3}H (tritium) for 2 min. Cultures were subsequently chased with non-labeled uracil and samples were collected at the indicated times. At each time point, the rRNA was extracted and resolved in 8% urea + 4% polyacrylamide gels by electrophoresis. The radiogram of the gels shows that initially only the 17S rRNA precursor is detected, but it is processed and converted to 16S rRNA in ∼25 min for the wild type strain and the Δ*rimM* strain containing an IPTG-inducible copy of *rimM*. In the case of the Δ*rimM* strain substantial levels of precursor rRNA and mature 16S rRNA are visible throughout the time course that had to be expanded to 120 min. (**C**) Equivalent pulse-chase labeling experiment performed with the Δ*yjeQ* strain. The asterisk indicates an additional band that represents an aberrantly processed rRNA that typically appears in this strain.

to mature subunits we should observe the time-dependent loss of labeled 17S rRNA and the simultaneous appearance of labeled 16S rRNA.

In the wild-type strain, the radiolabeled rRNA showed a rapid, monotonic disappearance of the 17S rRNA band with the concomitant emergence of the 16S rRNA band, consistent with rapid conversion of the immature species to the mature form in wild-type cells. Nearly all of the labeled 17S rRNA was converted to 16S rRNA in approximately 15 min of the initial pulse (Figure 1B, top panel). In Δ*rimM* (Figure 1B) and Δ*yjeQ* (Figure 1C) cells, the 17S rRNA persists substantially longer than it did in the parental strain. Even after 2 h of growth ∼50% of the initial 17S rRNA was still present in both null strains. There was, however, a clear emergence of 16S rRNA over the course of growth suggesting that a substantial proportion of the immature particles progress to fully mature 30S ribosomes. To corroborate that the delay on the processing of the 17S rRNA in the null strains was caused by the absence of YjeQ or RimM, the null strains were transformed with an IPTG-inducible copy of the *yje*Q and *rimM* gene, respectively. Expression of these genes was initiated with 10 μM IPTG at the beginning of the 'chase' phase of the experiment. The transformed null strains showed almost a complete processing of the radiolabeled 17S rRNA to 16S rRNA in an incubation time similar to the parental strain (Figure 1B and C). Transforming the Δ*rimM* and Δ*yjeQ* strains with the empty IPTG-inducible vector also showed slow processing of the 17S rRNA into 16S rRNA, similar to the assembly factor knockout strains with no overexpression plasmid (Figure 1B and C).

Overall these data were consistent with the progression of at least ∼50% of the $30S_{\Delta yjeQ}$ or $30S_{\Delta rimM}$ immature particles that accumulate in the Δ*rimM* and Δ*yjeQ* strains into mature 30S subunits. The remaining particles may eventually undergo transformation into mature particles beyond the two hours incubation of our assay or alternatively, represent dead-end products of the assembly process that are eventually degraded.

Immature 30S ribosomal subunits that accumulate in the *ΔrimM and ΔyjeQ strains* progress into 30S subunits that can bind 50S particles

Additional evidence that at least a significant percentage of the immature 30S ribosomal particles accumulating in Δ*rimM* and Δ*yjeQ* strains progress to the mature state was obtained by performing *in vitro* maturation assays with cell lysates obtained from the Δ*yjeQ* and Δ*rimM* strains (Figure 2). Previous structural characterization of these immature 30S particles in Δ*rimM* and Δ*yjeQ* strains have revealed that essential inter-subunit bridges (B2a and B3) and the 3′ minor domain are present in a distorted, flexible conformation that prevents their association with the 50S subunit (22,24,27,29). Therefore, in these assays we tested whether the assembling 30S particles that accumulate in the null strains are able to mature by measuring the ability of 30S particles to form 70S ribosomes upon different incubation conditions of the cell lysates. The premise of this assay was that only the 30S subunits that adopt a mature structure would be able to associate with 50S subunits to form 70S ribosomes.

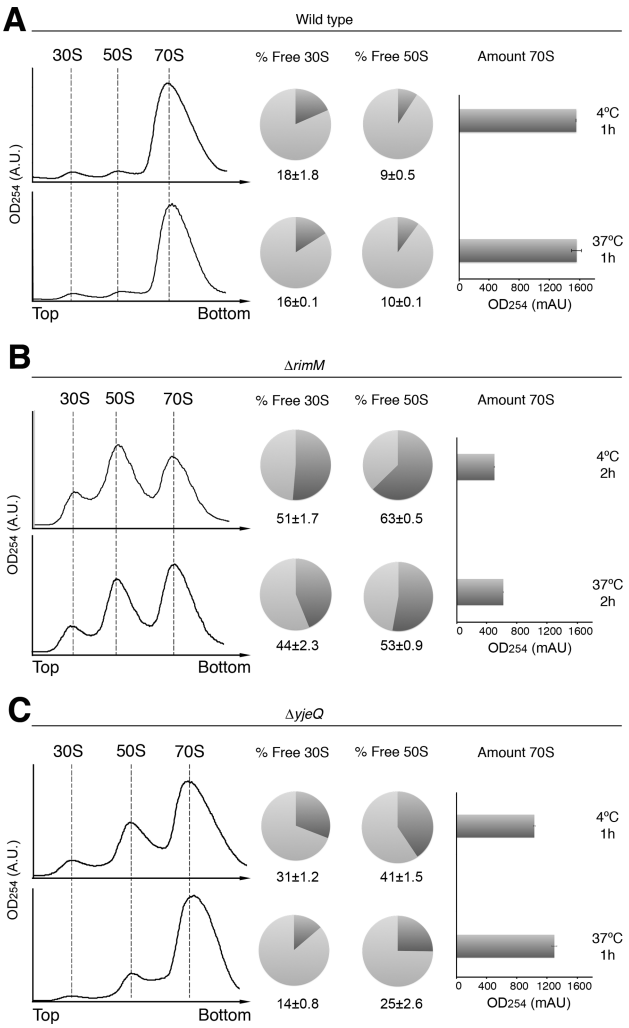

Figure 2. The immature $30S_{\Delta yjeQ}$ or $30S_{\Delta rimM}$ particles are able to associate with 50S subunits to form 70S ribosomes. Concentrated cell lysates of wild type (**A**), *rimM* (**B**) and *yjeQ* (**C**) null strains were incubated at either 37 °C or 4 °C for the specified time. After the treatment, crude ribosomes were purified from these cell extracts and layered onto sucrose gradients that separated the 30S and 50S subunits and the 70S ribosomes allowing for the distribution of each subunit to be calculated. Panels in the figures show the results for the wild type (A), Δ*rimM* strain (B) and Δ*yjeQ* (C) strains. The standard deviations shown correspond to three replicas of the experiment. We performed an unpaired t-test for each strain to determine the statistical significance of the changes observed in the percentages of free 30S and 50S subunits and amount of 70S ribosomes upon incubation. The obtained *P*-values for the changes during incubation in the free 30S, free 50S and total 70S ribosomes for wild type were $P > 0.05$. In the case of the Δ*yjeQ* strain the obtained *P*-values were $P < 0.0001$ (free 30S) and $P < 0.001$ (free 50S and 70S). Finally for the Δ*rimM* strain *P*-values were $P < 0.05$ (free 30S) and $P < 0.0001$ (free 50S and 70S).

Cell lysates were obtained from exponentially growing wild type, Δ*yje*Q and Δ*rim*M strains. The cell lysates were then concentrated in a centrifugal device, incubated for 1 h at 4°C or at 37°C, separated by sucrose gradient ultracentrifugation and the distribution of free 30S and 50S subunits and the amount of 70S ribosomes was analyzed (Figure 2).

Incubation of cell lysates from wild-type cells at 37°C for 1 h led to no substantial change in the amount of free 30S

and 50S subunits or 70S ribosomes compared to a control where the incubation was done at 4°C for 1 h (Figure 2A). This control experiment ensures that concentration and incubation of the cell lysates did not alter the distribution of particles in the ribosome profile, increase the amount of 70S ribosomes or cause degradation of subunits.

Concentration of cell lysates from the Δ*rimM* (Figure 2B) and Δ*yjeQ* (Figure 2C) strains led to a substantial reduction in the amount of free 30S and 50S subunits and a concurrent increase in the amount of 70S ribosomes when incubated at 37°C compared to 4°C. The percentage of free 30S subunits in the Δ*yjeQ* strain when cell lysates were maintained at 4°C was 31% and decreased to 14% upon incubation at 37°C. Similarly for the free 50S subunits, their percentage also decreased from 41% to 25%, and the amount of 70S ribosomes increased by 25% (Figure 2C). In the case of the Δ*rimM* strain we found that 1 h incubation at 37°C only induced a minor effect on the distribution of ribosomal particles of the cell lysates compared to the 4°C control (data not shown). However, when the incubation time was increased to 2 h we also saw the percentages of free 30S subunits decrease from 51% to 44%. The percentage of 50S subunits also decreased and the amount of 70S ribosomes increased by 24% at 37°C versus 4°C (Figure 2B).

These results along with the pulse-chase experiments suggest that a significant percentage (∼50%) of the immature 30S subunits that accumulate in the null strains are competent for maturation. In these cells the remaining assembly factors seem to be able to drive the maturation of the immature particles. It is also plausible that the maturation in the absence of YjeQ or RimM is factor independent. In any event, in the absence of these factors maturation occurs at a much slower rate.

The immature $30S_{\Delta yjeQ}$ and $30S_{\Delta rimM}$ particles accumulating in bacterial cells have substoichiometric amounts of YjeQ, Era, RimM and RbfA bound

To determine the occupancy level of YjeQ, Era, RimM and RbfA in the immature particles and mature 30S subunit *in vivo*, we purified mature 30S subunits from wild-type cells, and immature $30S_{\Delta yjeQ}$ and $30S_{\Delta rimM}$ particles from the null strains using a modified low-salt purification procedure. By working under these low-salt conditions (60 mM NH_4Cl), we hoped to maintain native interactions between the small subunit particles (SSU) and the assembly factors. The purified particles were then spiked with stoichiometric ^{15}N-labeled 70S ribosomes and purified assembly factors (Era, RbfA, RimM and YjeQ). Samples were digested with trypsin and peptide abundances were analyzed via quantitative mass spectrometry (qMS) using a targeted multiple reaction monitoring (MRM-HR) approach. To determine the reproducibility of our measurements, the immature subunits were assayed in duplicate.

Consistent with previous qMS analysis (22,24,27) both immature particles were severely depleted of r-protein uS2 and bS21 (40). A subtle depletion of uS3 was also observed in both immature particles. Additionally, the $30S_{\Delta rimM}$ particles were partially depleted of uS13 and uS14 in both replicates (Figure 3A). Notably, control reactions from wild-type strains with either mature 30S subunits or 70S particles exhibited stoichiometric binding of each small subunit r-protein. Given the low abundance of uS2 and bS21 in the immature small subunit particles, we next asked whether these proteins accumulated in the cell or, alternatively, how their abundance was regulated in the mutant strains.

To this end, we grew wild type (WT), Δ*rimM*, and Δ*yjeQ* strains in ^{14}N-labeled media. We then spiked these cell lysates as described above and measured the whole cell protein levels for small subunit ribosomal particles using qMS. Interestingly, we found that uS2 and bS21 were significantly depleted from the whole cell lysates (Figure 3B) indicating that these proteins, which are not bound to the immature particles, do not accumulate as free proteins in the cell. This whole cell depletion effect may result from downregulated synthesis or upregulated degradation of these particular proteins when they are not bound to a ribosomal particle. Interestingly, degradation of bS21 has been observed in wild-type cells previously (41). Additionally, we see more subtle depletion of proteins uS3, uS10, uS13, and uS14 specifically in the Δ*rimM* strain cell lysate.

We next extended our qMS method to measure the abundance of assembly factors Era, RbfA, RimM and YjeQ. To determine the linearity of our approach, we first titrated purified ^{14}N-labeled factors against a fixed concentration of ^{15}N-labeled factors in the presence of both ^{14}N- and ^{15}N-labeled 70S subunits. Plotting the ^{14}N-labeled protein added against the measured $^{14}N/^{15}N$ ratio revealed the linearity of the approach (Figure 3C). We then measured the factor occupancy in either purified subunits (Figure 3D) or in whole cell lysates (Figure 3E). With the exception of RbfA, factor, occupancy was extremely low and below our quantitation limit in all particles tested (∼5%). We found low but measurable (∼15%) occupancy of RbfA in the WT 30S and in the $30S_{\Delta rimM}$ particles. Additionally, RbfA was found at ∼5% occupancy in the $30S_{\Delta yjeQ}$particles as well as the wild type 70S.

Analysis of the protein levels in cell lysates of parental and null strains revealed that YjeQ, RbfA, RimM and Era are not highly abundant when immature particles accumulate in the cell (Figure 3E). Consistent with the factor occupancy levels found in the ribosomal particles purified under low salt buffer conditions, the measured protein levels in the cell lysates indicated that YjeQ, RimM and Era were present at levels less than 5% that of the total quantity of ribosomal proteins in the cell. In contrast, RbfA was present at higher levels in each strain although the overall abundance was still less than 10% of the total r-proteins. Taken together, the observed low factor abundance is consistent with recent protein abundance measures in wild-type cells by ribosome footprinting (42).

YjeQ binds to the mature 30S subunit with higher affinity than to the immature 30S particles

We first used pelleting assays to test the binding of YjeQ to the mature 30S subunit and to the $30S_{\Delta yjeQ}$ and $30S_{\Delta rimM}$ immature particles. To this end, we incubated in the presence of GMP–PNP, the assembly factors and ribosomal particles at a concentration of 7 and 1 μM, respectively. The premise of this assay is that any assembly factors that interact with the ribosome will pellet with the ribosomal par-

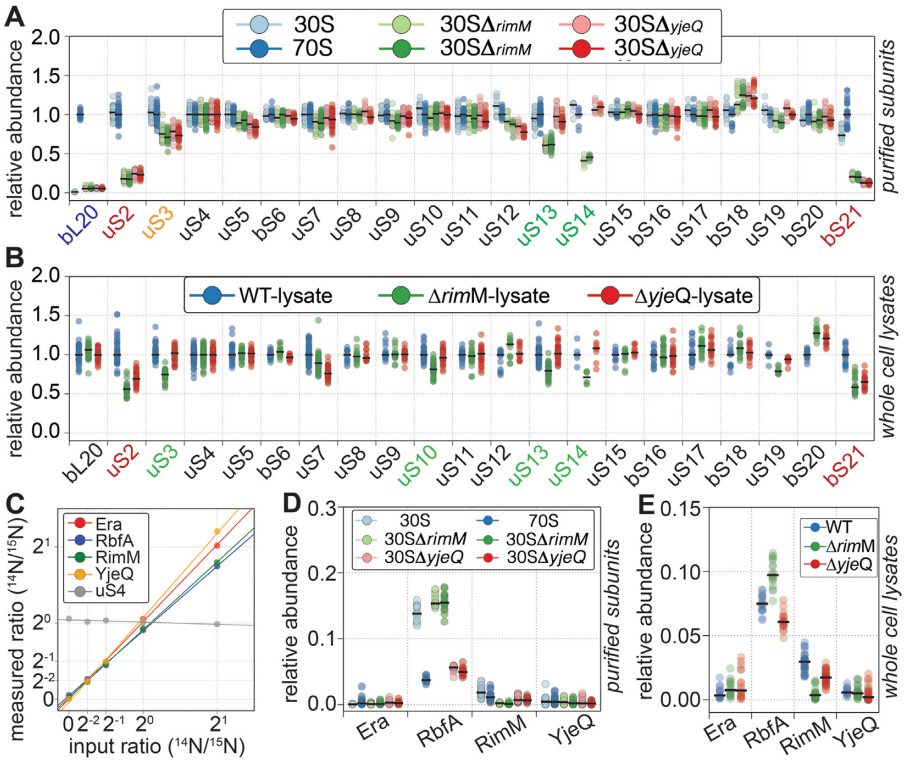

Figure 3. Ribosomal protein and assembly factor quantitation in mature and immature ribosomal particles. (**A**) ^{14}N-labeled subunits are quantified against a fixed ^{15}N-labeled 70S standard. Protein abundance is calculated as the ^{14}N/^{15}N ratio from extracted ion chromatograms of product ions, normalized to that of protein uS4. To highlight the different relative abundance of each protein relative to a fully mature 70S particle, for each protein, the abundance ratio is then normalized to that of the 70S ribosome. Circles denote a single product ion transition; black lines mark the median value. Replicates using 6 pmol or 12 pmol of 30S$_{\Delta rimM}$ (greens) and 30S$_{\Delta yjeQ}$ particles (reds) small subunits are plotted in light and dark colors respectively. Control mature 30S subunits and 70S ribosomes are shown in blues. Proteins significantly depleted from all immature subunits are labeled red, those slightly depleted are labeled orange and those specifically depleted in the 30S$_{\Delta rimM}$ particles are in green. For reference, a single large subunit protein is denoted with blue text. R-protein quantitation in whole cell lysates (**B**). ^{14}N-labeled whole cell lysates were spiked with ^{15}N-labeled 70S particles. ^{14}N/^{15}N relative abundance calculated from extracted ion chromatograms is normalized to that of protein uS4 and, to highlight strain specific differences, finally normalized relative to the wild-type lysate. Labels and colors are the same as in (A). Assembly factor quantitation calibration curve (**C**). Purified ^{14}N-labeled factors were added at various concentrations (0–12 pmol) to a fixed amount of purified ^{15}N-labeled factors (6 pmol) as well as both ^{14}N- and ^{15}N-labeled 70S particles (6 pmol each). For each targeted product ion transition, ion chromatograms were extracted for ^{14}N- and ^{15}N-labeled species. The median ratio is plotted for each protein at each measured concentration. Assembly factor quantitation in purified subunits (**D**) or in whole cell lysates (**E**). Samples prepared as described in (A) with the addition of ^{15}N-labeled purified assembly factors (6 pmol). Protein abundance determined and normalized as above (A) allowing for direct comparison between r-protein and assembly factor abundance.

ticles during centrifugation and any unbound factors will be retained in the supernatant. Supernatant and pellet were then collected and their content monitored by SDS-PAGE (Figure 4A). We found a band corresponding to YjeQ in the pelleting fraction of all the reactions containing ribosomal particles. Densitometry analysis determined that the intensity of this band was approximately three-fold stronger in the reaction with the mature 30S subunit compared to those containing the 30S$_{\Delta yjeQ}$ and 30S$_{\Delta rimM}$ immature particles. Instead, all of the YjeQ protein appeared in the flow through in the reaction containing no ribosomal particles. These results indicate that under these conditions YjeQ exhibits stronger binding affinity to the mature 30S subunit than to the immature particles.

We next used microscale thermophoresis (MST) to measure the dissociation constants (K_d values) of YjeQ binding to these ribosome particles. This technique has been shown to be a robust approach for measuring binding affinities in macromolecular assemblies made of proteins and DNA/RNA, including the ribosome (43,44). We fluorescently labeled the ribosomal particles on cysteine residues using the Red-Maleimide Protein Labeling Kit (NanoTemper Technologies) and tested that the labeling was not impeding YjeQ binding (Supplementary Figure S1). For each K_d measurement, YjeQ was titrated against a fixed concentration of the labeled 30S particles (40 nM) in the presence of GMP–PNP. After 10-min incubations, the reactions were loaded into hydrophobic MST capillaries and thermophoretic mobility of the fluorescently labeled ribosomal particles was analyzed. Consistent with the observations in the pelleting assays, YjeQ exhibited high binding affinity to the mature 30S subunit with a K_d value of ~66.2 ± 7.7 nM. However, it was not possible to reach saturation even at the highest YjeQ concentration tested (112 μM) when mixed with the 30S$_{\Delta yjeQ}$ and 30S$_{\Delta rimM}$ particles (Figure 4B). Consequently a K_d value for YjeQ binding to the immature particles was not obtained. These experiments suggested

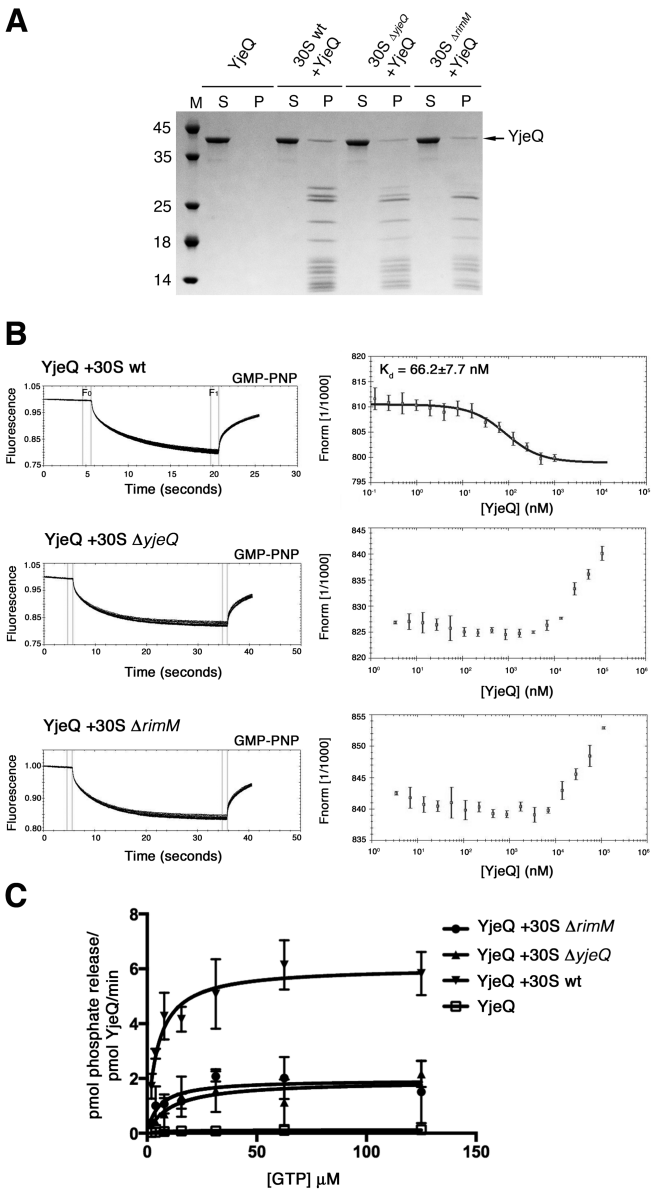

Figure 4. Binding of YjeQ to the mature and immature $30S_{\Delta yjeQ}$ and $30S_{\Delta rimM}$ particles. (**A**) Pelleting assay testing the binding of YjeQ to the mature and immature 30S particles. A sevenfold excess of YjeQ was incubated with either the mature 30S subunits or one of the immature 30S particles for 30 min at 37°C. Following the incubation, reactions were laid over a sucrose cushion and subjected to ultracentrifugation. Proteins that were unbound were collected in the supernatant (S), while proteins that bound to the 30S particle were found in the pellet (P). The molecular weight (M) is in kDa. The pellet and supernatant were resolved by 4–12% bis–tris SDS-PAGE and stained with Coomassie Brilliant Blue. The bands for YjeQ are indicated. (**B**) Analysis of the interactions of YjeQ with the mature 30S subunit and immature particles by MST in the presence of 1 mM GMP-PNP. In these experiments the concentration of the fluorescently labeled ribosomal particles was constant, while the concentration of unlabeled YjeQ was varied. After a short incubation the samples were loaded into MST hydrophobic glass capillaries, and the thermophoretic mobility of the labeled ribosomal particles (left panels) was measured using the Monolith.NT.115 instrument (NanoTemper). Measured changes in the MST response were used to produce curves that plotted the F_{norm} (‰) = F_1/F_0 versus YjeQ concentration. The F_1 and F_0 regions of the fluorescence time traces used to calculate F_{norm} (‰) are indicated in the panel. The F_{norm} (‰) curves were fit using the law of mass action to yield a K_d value. (**C**) Stimulation of the GTPase activity of YjeQ by the mature 30S subunit and immature $30S_{\Delta yjeQ}$ or $30S_{\Delta rimM}$ particles. The GTP hydrolysis rates of YjeQ in the presence and absence of the ribosomal particles were measured at different concentrations of GTP to determine steady-state kinetic parameters.

that the affinity of YjeQ to the immature particles is much weaker than to the mature 30S subunit.

To measure the effect of the nucleotide on the YjeQ K_d values, identical reactions were tested in the presence of GDP. In the reaction with the mature 30S subunit, binding of YjeQ was not detected at the highest concentration tested (4 μM), indicating a large drop in affinity with respect to the equivalent binding reaction in the presence of GMP–PNP. Binding of YjeQ to the immature particles was only detected at the highest concentrations of YjeQ tested (>112 μM), but it was not possible to saturate the binding reaction. These results indicate that in the presence of GDP, the binding affinity of YjeQ to the immature subunits is also extremely low (Supplementary Figure S2).

Next, we tested whether the binding of YjeQ to the mature 30S subunit at a protein concentration in the range of the K_d value obtained for the YjeQ+30S subunit complex constitutes a specific interaction. We also tested whether at this concentration range a specific interaction between YjeQ and the $30S_{\Delta yjeQ}$ and $30S_{\Delta rimM}$ particles is measurable. To this end, we took advantage of the low intrinsic GTPase activity of YjeQ, which increases upon specific interaction with ribosomal particles (45). In these experiments (Figure 4C), both the ribosomal particle and YjeQ were kept at 50 nM and the YjeQ GTPase activity was monitored with the malachite green assay at increasing concentrations of GTP. The GTPase activity exhibited by each ribosomal particle by itself at each GTP concentration was subtracted from the total GTPase activity measured in the corresponding reactions containing YjeQ and the ribosomal particles. This background subtraction ensured accuracy in the calculations by removing all background phosphate production not due to YjeQ. A steady-state kinetic analysis (Table 1) showed that YjeQ had a similar K_M for GTP when the protein was by itself or in the presence of any of the ribosomal particles. However, the GTPase activity, consistent with previous literature (45), exhibited a significant stimulation (>100-fold increase in k_{cat}/K_M) in the presence of the mature 30S subunit. Reactions containing immature $30S_{\Delta yjeQ}$ or $30S_{\Delta rimM}$ particles incubated with YjeQ also exhibited stimulation over the intrinsic YjeQ GTPase activity, albeit this stimulation was smaller (10–30-fold increase in k_{cat}/K_M) compared to that shown by the mature 30S subunit (Table 1).

Overall, our pelleting and MST experiments suggest that YjeQ is able to bind both the mature and immature 30S particles, however affinity for the mature 30S subunit is much higher than for the $30S_{\Delta yjeQ}$ or $30S_{\Delta rimM}$ particles. The GTPase assays establish that the observed interactions are specific as they trigger an enzymatic activity.

Table 1. Kinetic parameters of YjeQ in the presence and absence of the mature 30S subunit and immature $30S_{\Delta yjeQ}$ and $30S_{\Delta rimM}$ particles

	K_M (μM)	k_{cat} (h^{-1})	k_{cat}/K_M ($\mu M^{-1}\ h^{-1}$)	Increase in k_{cat}/K_M
YjeQ	10.07	0.1327	219.63	1
30S	4.474	6.059	2.256×10^4	103
$30S_{\Delta yjeQ}$	10.98	1.912	2.902×10^3	13
$30S_{\Delta rimM}$	5.36	1.949	6.060×10^3	27

Binding affinity of Era, RimM and RbfA to the mature 30S subunit and immature 30S particles is much weaker than that of YjeQ

To analyze the binding of Era to the mature 30S subunit and to the $30S_{\Delta yjeQ}$ and $30S_{\Delta rimM}$ particles, we used MST experiments and GTPase activity measurements. MST experiments (Figure 5A) revealed that the K_d of Era to the mature 30S subunit in the presence of GMPPNP was 7.3 ± 7.4 μM. This result is consistent with previous literature (46). Reactions to measure the K_d of this factor to the immature particles did not reach saturation at concentrations of Era as high as 42 μM. Thus, a K_d value for Era binding to the immature particles was not obtained. Performing the assembly reactions in the presence of GDP had no significant effect on the MST results for this factor (Supplementary Figure S3).

Finding that the binding affinity of Era to mature 30S subunit was much weaker than that of YjeQ, led us to test using GTPase assays whether at a protein concentration in the range of the K_d values obtained for the YjeQ + 30S complex (66.2 ± 7.7 nM) a specific interaction between Era and the ribosomal particles occurs (Figure 5B). Consistent with previous literature (47), Era was shown to have low intrinsic GTPase activity. In the steady-state kinetic analysis of this reaction, we used a GTP concentration range from 0 to 250 μM, which was the highest permitted concentration for the assay. The background of the assay itself was measured by running control reactions with only GTP and subsequently subtracting the background phosphate production from the total GTPase activity exhibited by the reactions containing the assembly factor. The reaction did not saturate and k_{cat} and K_M values could not be determined. Reactions containing Era at a 50 nM concentration and either mature or immature 30S particles at the same concentration did not show any enhancement of Era GTPase activity. Indeed, we did not detect any measurable phosphate being formed above background level (data not shown); thus a steady-state kinetic analysis for these reactions was not possible. Background subtraction of the GTPase activity exhibited by the ribosomal particles themselves was applied as in the assays with YjeQ.

In the case of RimM and RbfA, we initially tested their binding to the mature 30S subunits and to the $30S_{\Delta yjeQ}$ or $30S_{\Delta rimM}$ immature particles by filtration assays (Figure 5C). In these assays, despite the concentration of RbfA or RimM in the reaction being 2 μM, only a weak interaction of RbfA with the mature 30S subunit and the $30S_{\Delta rimM}$ immature particle was observed. This factor did not appreciably bind the $30S_{\Delta yjeQ}$ immature particle. In the case of RimM, we did not observe appreciable binding to any of the ribosomal particles. Consistent with the filtration assays, MST experiments used to measure the K_d values of

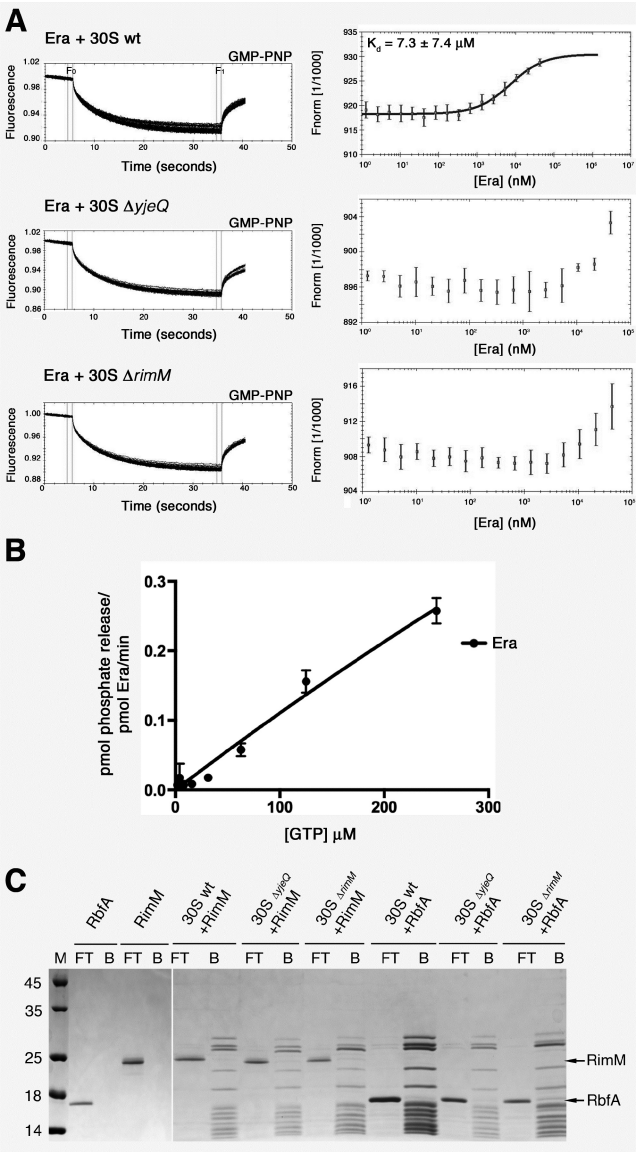

Figure 5. Binding of Era, RbfA and RimM to the mature 30S and immature $30S_{\Delta yjeQ}$ and $30S_{\Delta rimM}$ particles. (**A**) Analysis of the interactions of Era with the mature and immature $30S_{\Delta yjeQ}$ the $30S_{\Delta rimM}$ particles by MST. Interactions were measured in buffer containing GMP-PNP. Fluorescence time traces (left panel) and derived F_{norm} (‰) = F_1/F_0 curves (right panels) for the three binding reactions are shown. (**B**) Intrinsic GTPase activity of Era at different concentrations of GTP. (**C**) Coomassie Brilliant Blue stained 4–12% Bis–Tris polyacrylamide gels showing the content of the flow-through (FT) and bound (B) fractions of the filtration assay testing the binding of RimM and RbfA to the mature 30S and immature $30S_{\Delta yjeQ}$ and $30S_{\Delta rimM}$ particles. Reactions containing one of the factors alone or a mixture of five-fold molar excess of the factor and one of the ribosomal particles were incubated for 30 min at 37°C. Following incubation, the reactions were passed through a 100 kDa cut-off filter using centrifugation to obtain the FT and B fractions. The molecular weight (M) is in kDa.

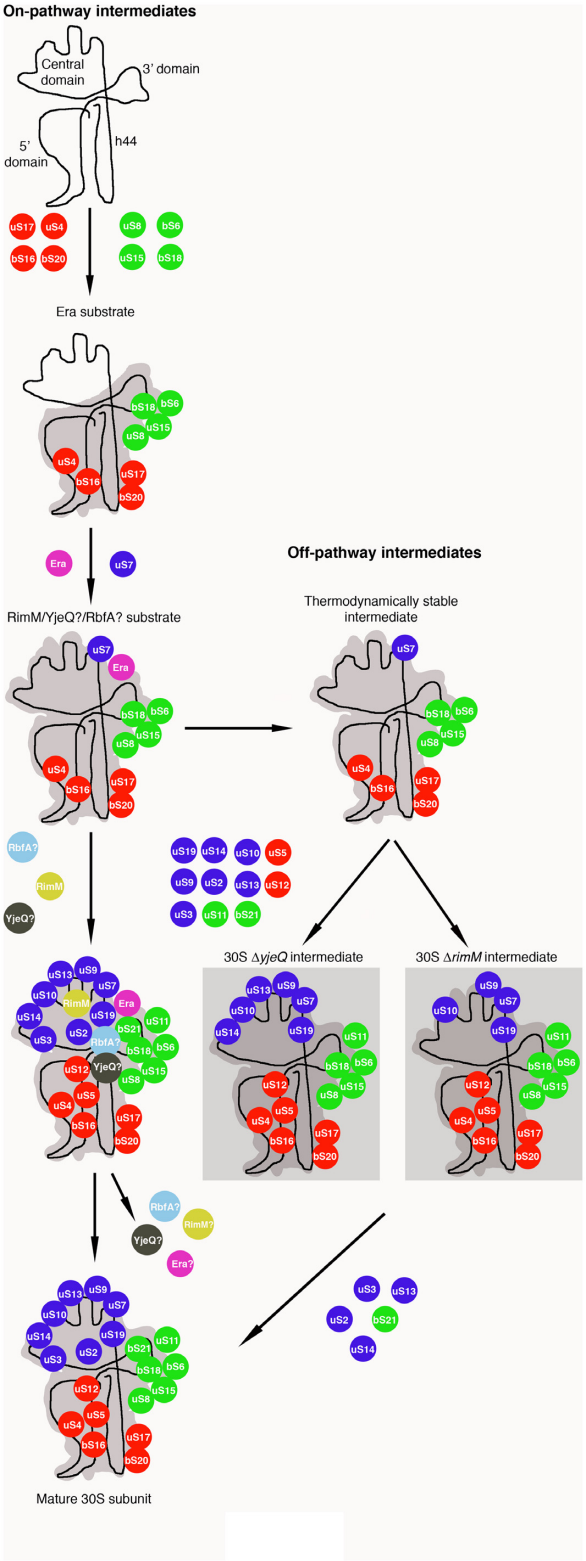

Figure 6. Model describing the placement of the $30S_{\Delta yjeQ}$ or $30S_{\Delta rimM}$ immature particles in the assembly pathway of the 30S subunit. The four domains of the 16S rRNA are labeled in the top left cartoon. Ribosomal proteins that belong to the 5′, central and 3′ domains are colored in red, green and blue, respectively. The entry of the r-proteins in the cartoon is shown according to the Nomura assembly map. Era and RimM point of entry in the assembly line is marked according to previous work (21) that helps define the actual substrate for these two factors (semi-transparent boxes). Points of entry for RbfA and YjeQ are displayed arbitrarily (denoted with a '?') as they are unknown. Similarly the release point of the four factors has been displayed arbitrarily as it is also unknown (denoted with a '?'). In the presence of YjeQ, RbfA, RimM and Era assembly progresses through on-pathway intermediates recognized by the factors until the mature 30S subunit is formed. In the absence of the assembly factors, the immature particles evolve into a more energetically stable folding state (labeled as 'Thermodynamically stable intermediate'). This intermediate continues to incorporate most of the remaining r-proteins except those that we found depleted in our qMS analysis and evolves into the $30S_{\Delta yjeQ}$ or $30S_{\Delta rimM}$ immature particles (highlighted by semi-transparent boxes) that accumulate and exhibit low affinity for the assembly factors. These accumulated particles can eventually mature into complete 30S subunits.

RbfA and RimM to the ribosomal particles (Supplementary Figure S4) found that none of the reactions reached saturation in spite of using concentrations of RimM and RbfA of 217 μM and 1 mM, respectively. Therefore, a K_d value for binding of RimM and RbfA to the immature particles was not obtained.

Overall, these experiments revealed that the binding affinity of Era, RimM and RbfA to both the mature 30S subunits and immature particles is much weaker than that of YjeQ to the mature 30S subunit. Similarly to YjeQ, the affinity of Era to the immature particles is much lower than to the mature 30S subunit.

DISCUSSION

An experimental approach extensively used by multiple groups (22,27–30,35) to gain new insights about the ribosome assembly process has been the use of single knockout or depletion strains that lack one of the protein factors assisting this process. These cells accumulate immature ribosomal particles that are informative on the reactions catalyzed by these assembly factors. Two main conclusions that came out from the analysis of these particles was that YjeQ, RbfA and RimM act at the late stages of assembly of the 30S subunit and that they assist the maturation of the functional core of the 30S subunit (22,27,29,46). Despite the increasing amount of literature on the roles of these assembly factors, how each protein assists in this process and their mechanistic details have not been described.

In this work, we provide evidence suggesting that at least ∼50% of the immature $30S_{\Delta yjeQ}$ and $30S_{\Delta rimM}$particles accumulating in the Δ*rimM* and Δ*yjeQ* null strains progress to mature 30S subunits. This finding provides reassurance that analysis of the immature 30S particles that accumulate in the Δ*rimM* and Δ*yjeQ* strains renders physiologically relevant information about the late stages of assembly facilitated by YjeQ and RimM. Interestingly, we found that YjeQ and Era bind to the mature 30S subunit with high affinity, but their binding affinity to $30S_{\Delta yjeQ}$ and $30S_{\Delta rimM}$ was much lower. For Era binding to the immature particles is not occurring at physiological concentrations and for RimM and RbfA, we found that their binding affinity to the 30S subunit and immature subunits was either weak or binding was not detected.

Consistent with these affinity measurements, we found substoichiometric occupancy of YjeQ, Era, RbfA and RimM in the immature 30S particles that accumulate in null

cells. These results are also in agreement with existing cryo-electron microscopy structures proving a stable interaction of YjeQ (23,24), Era (26) or RbfA (31) with mature 30S subunit. In these structural studies, protein concentrations in the micromolar range were used to assemble and visualize these complexes. These are protein concentrations at which our experiments (Figures 4 and 5) also detected an interaction between YjeQ, Era or RbfA and mature 30S subunits.

Considering that YjeQ, RbfA, RimM and Era are putative assembly factors, the weak binding of these factors to the immature particles was an unexpected result. However, this result reconciles well with a putative role of these factors in chaperoning the folding of rRNA. Similarly to the r-proteins that upon binding to the rRNA stabilize transient RNA conformations and keep the rRNA in a productive line of folding, it is likely that YjeQ, RbfA, RimM and Era may also play a role in stabilizing specific rRNA motifs at or near the decoding center in certain conformations (23,24,26,31,48). In the absence of any of these factors, the conformation of the rRNA motifs that these factors should bind may transition into a local energy minimum that is thermodynamically more stable. Our current thinking is that in the knockout strains the on-pathway intermediate that constitute the real substrate for each factor progresses to a downstream assembly intermediate that exhibits low affinity to the factors. Indeed, recent studies (22,27–29) found that the $30S_{\Delta yjeQ}$ and $30S_{\Delta rimM}$particles accumulating in the Δ*rimM* and Δ*yjeQ* null strains are structurally similar. Therefore, it seems that in the knockout strains the different on-pathway intermediates that are recognized by the specific assembly factors may be progressing into a structurally similar local energy minimum intermediate.

These results imply that the true substrates of YjeQ, RbfA, RimM and Era are assembling particles that precede the immature intermediates accumulating in the knockout strains. This is consistent with recent work (21) testing the effect of Era and RimM on the kinetics of incorporation of r-proteins to the assembling 30S subunit *in vitro*. This study found that Era causes acceleration of the binding rates of r-proteins uS5, uS9, uS11 and uS12. There was also a more subtle increase in the kinetics of incorporation of uS7, uS10, uS13, uS14 and uS19. RimM affected the kinetics of incorporation of r-proteins uS3, uS9, uS10, uS12, uS13 and uS19. This study along with the Nomura assembly map (49–51), establishing the hierarchy of binding of the r-proteins, allows one to estimate a point of entry of Era and RimM into the assembly line of the 30S subunit (Figure 6). The qMS analysis presented here (Figure 3) also allowed us to put an estimated time stamp on the $30S_{\Delta yjeQ}$ and $30S_{\Delta rimM}$ immature particles and position them within this assembly line. All of the r-proteins with incorporation kinetics that are affected by the presence of Era or RimM (21) were present in the immature particles in full occupancy. The only exceptions were uS3 that was partially depleted in both particles and uS13 and uS14 were slightly depleted in the $30S_{\Delta rimM}$ particles. This protein complement placed the $30S_{\Delta yjeQ}$ or $30S_{\Delta rimM}$ immature particles that accumulate in the Δ*yje*Q and Δ*rimM* null strains at the very late stages of the assembly pathway and more importantly, downstream of the particles recognized by YjeQ and RimM as substrates. Our current hypothesis is that the thermodynamically more stable intermediate to which the true substrate particle for RimM and YjeQ evolve to (labeled as 'Thermodynamically stable intermediate' in Figure 6), still continues to incorporate most of the remaining r-proteins except those that we found depleted in our qMS analysis (Figure 3). These are the $30S_{\Delta yjeQ}$ or $30S_{\Delta rimM}$ immature particles that accumulate in the *yjeQ* and *rimM* null strains (shown enclosed in a semi-transparent box in Figure 6). Data presented here also indicates that these immature particles have the ability to progress into 30S subunits that can associate with 50S subunits and form fully assemble 70S ribosomes.

In conclusion, this study brings new insights into the nature of the immature ribosomal particles that assembly factor single knockout strains accumulate and the information that their study provides about the maturation reaction catalyzed by these factors.

SUPPLEMENTARY DATA

Supplementary Data are available at NAR Online.

ACKNOWLEDGEMENTS

We are grateful to Dr Dinorah Leyva and Christine Lai for assistance with the microscale thermophoresis experiments. We also thank Drs Eric Brown and Geordie Stewart for stimulating discussions in this project. The funders had no role in study design, data collection and analysis, decision to publish, or preparation of the manuscript.

FUNDING

National Science and Engineering Research Council of Canada [RGPIN288327-07]; Canadian Institutes of Health Research [MOP-82930 to J.O., a NSERC-RTI (EQPEQ45847) to T.F.M.]; National Institutes of Health [R37-GM-053757 to J.R.W.]; Jane Coffin Childs Postdoctoral fellowship and a grant from the National Institute of Aging [1K99AG050749-01 to J.H.D.]. Funding for open access charge: Canadian Institutes of Health Research.
Conflict of interest statement. None declared.

REFERENCES

1. Wimberly,B.T., Brodersen,D.E., Clemons,W.M. Jr, Morgan-Warren,R.J., Carter,A.P., Vonrhein,C., Hartsch,T. and Ramakrishnan,V. (2000) Structure of the 30S ribosomal subunit. *Nature*, **407**, 327–339.
2. Culver,G.M. (2003) Assembly of the 30S ribosomal subunit. *Biopolymers*, **68**, 234–249.
3. Ramakrishnan,V. (2002) Ribosome structure and the mechanism of translation. *Cell*, **108**, 557–572.
4. Harms,J., Schluenzen,F., Zarivach,R., Bashan,A., Gat,S., Agmon,I., Bartels,H., Franceschi,F. and Yonath,A. (2001) High resolution structure of the large ribosomal subunit from a mesophilic eubacterium. *Cell*, **107**, 679–688.
5. Ban,N., Nissen,P., Hansen,J., Moore,P.B. and Steitz,T.A. (2000) The complete atomic structure of the large ribosomal subunit at 2.4 A resolution. *Science*, **289**, 905–920.
6. Bashan,A., Agmon,I., Zarivach,R., Schluenzen,F., Harms,J., Berisio,R., Bartels,H., Franceschi,F., Auerbach,T., Hansen,H.A. *et al.* (2003) Structural basis of the ribosomal machinery for peptide bond formation, translocation, and nascent chain progression. *Mol. Cell*, **11**, 91–102.

7. Frank,J. (2003) Toward an understanding of the structural basis of translation. *Genome Biol.*, **4**, 237.
8. Shajani,Z., Sykes,M.T. and Williamson,J.R. (2011) Assembly of bacterial ribosomes. *Annu. Rev. Biochem.*, **80**, 501–526.
9. Sykes,M.T. and Williamson,J.R. (2009) A Complex Assembly Landscape for the 30S Ribosomal Subunit. *Annu. Rev. Biophys.*, **38**, 197–215.
10. Woodson,S.A. (2008) RNA folding and ribosome assembly. *Curr. Opin. Chem. Biol.*, **12**, 667–673.
11. Woodson,S.A. (2011) RNA folding pathways and the self-assembly of ribosomes. *Accounts Chem. Res.*, **44**, 1312–1319.
12. Decatur,W.A. and Fournier,M.J. (2002) rRNA modifications and ribosome function. *Trends Biochem. Sci.*, **27**, 344–351.
13. Dahlberg,A.E., Dahlberg,J.E., Lund,E., Tokimatsu,H., Rabson,A.B., Calvert,P.C., Reynolds,F. and Zahalak,M. (1978) Processing of the 5′ end of Escherichia coli 16S ribosomal RNA. *Proc. Natl. Acad. Sci. U.S.A.*, **75**, 3598–3602.
14. Kurata,T., Nakanishi,S., Hashimoto,M., Taoka,M., Yamazaki,Y., Isobe,T. and Kato,J. (2015) Novel essential gene Involved in 16S rRNA processing in Escherichia coli. *J. Mol. Biol.*, **427**, 955–965.
15. Li,Z., Pandit,S. and Deutscher,M.P. (1999) RNase G (CafA protein) and RNase E are both required for the 5′ maturation of 16S ribosomal RNA. *EMBO J.*, **18**, 2878–2885.
16. Sulthana,S. and Deutscher,M.P. (2013) Multiple exoribonucleases catalyze maturation of the 3′ terminus of 16S ribosomal RNA (rRNA). *J. Biol. Chem.*, **288**, 12574–12579.
17. Adilakshmi,T., Bellur,D.L. and Woodson,S.A. (2008) Concurrent nucleation of 16S folding and induced fit in 30S ribosome assembly. *Nature*, **455**, 1268–1272.
18. Bunner,A.E., Beck,A.H. and Williamson,J.R. (2010) Kinetic cooperativity in Escherichia coli 30S ribosomal subunit reconstitution reveals additional complexity in the assembly landscape. *Proc. Natl. Acad. Sci. U.S.A.*, **107**, 5417–5422.
19. Mulder,A.M., Yoshioka,C., Beck,A.H., Bunner,A.E., Milligan,R.A., Potter,C.S., Carragher,B. and Williamson,J.R. (2010) Visualizing ribosome biogenesis: parallel assembly pathways for the 30S subunit. *Science*, **330**, 673–677.
20. Talkington,M.W., Siuzdak,G. and Williamson,J.R. (2005) An assembly landscape for the 30S ribosomal subunit. *Nature*, **438**, 628–632.
21. Bunner,A.E., Nord,S., Wikstrom,P.M. and Williamson,J.R. (2010) The effect of ribosome assembly cofactors on in vitro 30S subunit reconstitution. *J. Mol. Biol.*, **398**, 1–7.
22. Jomaa,A., Stewart,G., Martin-Benito,J., Zielke,R., Campbell,T.L., Maddock,J.R., Brown,E.D. and Ortega,J. (2011) Understanding ribosome assembly: the structure of in vivo assembled immature 30S subunits revealed by cryo-electron microscopy. *RNA*, **17**, 697–709.
23. Jomaa,A., Stewart,G., Mears,J.A., Kireeva,I., Brown,E.D. and Ortega,J. (2011) Cryo-electron microscopy structure of the 30S subunit in complex with the YjeQ biogenesis factor. *RNA*, **17**, 2026–2038.
24. Guo,Q., Yuan,Y., Xu,Y., Feng,B., Liu,L., Chen,K., Sun,M., Yang,Z., Lei,J. and Gao,N. (2011) Structural basis for the function of a small GTPase RsgA on the 30S ribosomal subunit maturation revealed by cryoelectron microscopy. *Proc. Natl. Acad. Sci. U.S.A.*, **108**, 13100–13105.
25. Bylund,G.O., Wipemo,L.C., Lundberg,L.A. and Wikstrom,P.M. (1998) RimM and RbfA are essential for efficient processing of 16S rRNA in Escherichia coli. *J. Bacteriol.*, **180**, 73–82.
26. Sharma,M.R., Barat,C., Wilson,D.N., Booth,T.M., Kawazoe,M., Hori-Takemoto,C., Shirouzu,M., Yokoyama,S., Fucini,P. and Agrawal,R.K. (2005) Interaction of Era with the 30S ribosomal subunit implications for 30S subunit assembly. *Mol. Cell*, **18**, 319–329.
27. Leong,V., Kent,M., Jomaa,A. and Ortega,J. (2013) Escherichia coli rimM and yjeQ null strains accumulate immature 30S subunits of similar structure and protein complement. *RNA*, **19**, 789–802.
28. Guo,Q., Goto,S., Chen,Y., Feng,B., Xu,Y., Muto,A., Himeno,H., Deng,H., Lei,J. and Gao,N. (2013) Dissecting the in vivo assembly of the 30S ribosomal subunit reveals the role of RimM and general features of the assembly process. *Nucleic Acids Res.*, **41**, 2609–2620.
29. Yang,Z., Guo,Q., Goto,S., Chen,Y., Li,N., Yan,K., Zhang,Y., Muto,A., Deng,H., Himeno,H. *et al.* (2014) Structural insights into the assembly of the 30S ribosomal subunit in vivo: functional role of S5 and location of the 17S rRNA precursor sequence. *Protein Cell*, **5**, 394–407.
30. Clatterbuck Soper,S.F., Dator,R.P., Limbach,P.A. and Woodson,S.A. (2013) In vivo X-ray footprinting of pre-30S ribosomes reveals chaperone-dependent remodeling of late assembly intermediates. *Mol. Cell*, **52**, 506–516.
31. Datta,P.P., Wilson,D.N., Kawazoe,M., Swami,N.K., Kaminishi,T., Sharma,M.R., Booth,T.M., Takemoto,C., Fucini,P., Yokoyama,S. *et al.* (2007) Structural aspects of RbfA action during small ribosomal subunit assembly. *Mol. Cell*, **28**, 434–445.
32. Baba,T., Ara,T., Hasegawa,M., Takai,Y., Okumura,Y., Baba,M., Datsenko,K.A., Tomita,M., Wanner,B.L. and Mori,H. (2006) Construction of Escherichia coli K-12 in-frame, single-gene knockout mutants: the Keio collection. *Mol. Syst. Biol.*, **2**, 2006 0008.
33. Kitagawa,M., Ara,T., Arifuzzaman,M., Ioka-Nakamichi,T., Inamoto,E., Toyonaga,H. and Mori,H. (2005) Complete set of ORF clones of Escherichia coli ASKA library (a complete set of E. coli K-12 ORF archive): unique resources for biological research. *DNA Res.*, **12**, 291–299.
34. Jeganathan,A., Razi,A., Thurlow,B. and Ortega,J. (2015) The C-terminal helix in the YjeQ zinc-finger domain catalyzes the release of RbfA during 30S ribosome subunit assembly. *RNA*, **21**, 1203–1216.
35. Jomaa,A., Jain,N., Davis,J.H., Williamson,J.R., Britton,R.A. and Ortega,J. (2014) Functional domains of the 50S subunit mature late in the assembly process. *Nucleic Acids Res.*, **42**, 3419–3435.
36. MacLean,B., Tomazela,D.M., Shulman,N., Chambers,M., Finney,G.L., Frewen,B., Kern,R., Tabb,D.L., Liebler,D.C. and MacCoss,M.J. (2010) Skyline: an open source document editor for creating and analyzing targeted proteomics experiments. *Bioinformatics*, **26**, 966–968.
37. Stokes,J.M., Davis,J.H., Mangat,C.S., Williamson,J.R. and Brown,E.D. (2014) Discovery of a small molecule that inhibits bacterial ribosome biogenesis. *eLife*, **3**, e03574.
38. Gulati,M., Jain,N., Davis,J.H., Williamson,J.R. and Britton,R.A. (2014) Functional interaction between ribosomal protein L6 and RbgA during ribosome assembly. *PLoS Genet.*, **10**, e1004694.
39. Himeno,H., Hanawa-Suetsugu,K., Kimura,T., Takagi,K., Sugiyama,W., Shirata,S., Mikami,T., Odagiri,F., Osanai,Y., Watanabe,D. *et al.* (2004) A novel GTPase activated by the small subunit of ribosome. *Nucleic Acids Res.*, **32**, 5303–5309.
40. Ban,N., Beckmann,R., Cate,J.H., Dinman,J.D., Dragon,F., Ellis,S.R., Lafontaine,D.L., Lindahl,L., Liljas,A., Lipton,J.M. *et al.* (2014) A new system for naming ribosomal proteins. *Curr. Opin. Struct. Biol.*, **24**, 165–169.
41. Chen,S.S., Sperling,E., Silverman,J.M., Davis,J.H. and Williamson,J.R. (2012) Measuring the dynamics of E. coli ribosome biogenesis using pulse-labeling and quantitative mass spectrometry. *Mol. Biosyst.*, **8**, 3325–3334.
42. Li,G.W., Burkhardt,D., Gross,C. and Weissman,J.S. (2014) Quantifying absolute protein synthesis rates reveals principles underlying allocation of cellular resources. *Cell*, **157**, 624–635.
43. Zillner,K., Jerabek-Willemsen,M., Duhr,S., Braun,D., Langst,G. and Baaske,P. (2012) Microscale thermophoresis as a sensitive method to quantify protein: nucleic acid interactions in solution. *Methods Mol. Biol.*, **815**, 241–252.
44. Godinic-Mikulcic,V., Jaric,J., Greber,B.J., Franke,V., Hodnik,V., Anderluh,G., Ban,N. and Weygand-Durasevic,I. (2014) Archaeal aminoacyl-tRNA synthetases interact with the ribosome to recycle tRNAs. *Nucleic Acids Res.*, **42**, 5191–5201.
45. Daigle,D.M., Rossi,L., Berghuis,A.M., Aravind,L., Koonin,E.V. and Brown,E.D. (2002) YjeQ, an essential, conserved, uncharacterized protein from Escherichia coli, is an unusual GTPase with circularly permuted G-motifs and marked burst kinetics. *Biochemistry*, **41**, 11109–11117.
46. Sayed,A., Matsuyama,S. and Inouye,M. (1999) Era, an essential Escherichia coli small G-protein, binds to the 30S ribosomal subunit. *Biochem. Biophys. Res. Commun.*, **264**, 51–54.
47. Johnstone,B.H., Handler,A.A., Chao,D.K., Nguyen,V., Smith,M., Ryu,S.Y., Simons,E.L., Anderson,P.E. and Simons,R.W. (1999) The widely conserved Era G-protein contains an RNA-binding domain required for Era function in vivo. *Mol. Microbiol.*, **33**, 1118–1131.
48. Lovgren,J.M., Bylund,G.O., Srivastava,M.K., Lundberg,L.A., Persson,O.P., Wingsle,G. and Wikstrom,P.M. (2004) The PRC-barrel domain of the ribosome maturation protein RimM mediates binding

to ribosomal protein S19 in the 30S ribosomal subunits. *RNA*, **10**, 1798–1812.
49. Traub,P. and Nomura,M. (1968) Structure and function of E. coli ribosomes. V. Reconstitution of functionally active 30S ribosomal particles from RNA and proteins. *Proc. Natl. Acad. Sci. U.S.A.*, **59**, 777–784.
50. Traub,P. and Nomura,M. (1969) Structure and function of Escherichia coli ribosomes. VI. Mechanism of assembly of 30 s ribosomes studied in vitro. *J. Mol . Biol.*, **40**, 391–413.
51. Traub,P. and Nomura,M. (1969) Studies on the assembly of ribosomes in vitro. *Cold Spring Harb. Symp. Quant. Biol.*, **34**, 63–67.